A Soft Unmanned Underwater Vehicle with augmented thrust capability

Francesco Giorgio-Serchi, Andrea Arienti and Cecilia Laschi
Centre for Sea Technologies and Marine Robotics
The BioRobotics Institute
Scuola Superiore Sant'Anna
Livorno, Italy, 57126
Email: f.serchi@sssup.it, a.arienti@sssup.it, c.laschi@sssup.it

***Abstract*—The components which could make Soft Unmanned Underwater Vehicles a winning technology for a range of marine operations are addressed: these include vortex-enhanced thrust, added mass recovery and high degree of compliance of the vehicle. Based on these design criteria and recent advancement in soft-bodied, pulsed-jet thrusters, a new underwater vehicle is developed and tested.**

I. Introduction

Now more than ever since the time of their appearance, Autonomous Underwater Vehicles (AUVs) and Remotely Operated Vehicles (ROVs) are required to perform more complex tasks in more extreme conditions, [1].

Two of the limitations of current ROVs, which will be addressed in this paper, are their bulk/ruggedness and their manoeuvrability. ROVs must avoid impacts because, due to their structure, they might cause or suffer damages. This stands true in particular for those scenarios where manipulator-endowed ROVs, or UVMSs (Underwater Vehicle Manipulator Systems) [2], are required to perform maintenance/construction tasks in unstructured and highly perturbed environments. In such hostile conditions, ROVs and UVMSs need to rely on a very accurate control which manages the positioning, collision avoidance, the contact problem, etc. and at the same time exploit their high inertia and multiple thrusters to minimize external perturbations and perform highly non-stationary manoeuvring. These are extremely challenging tasks even for land-based robots, but in the submerged world, some of these issues become overwhelming due to a series of major complications summarised herein. One bottle neck of underwater robot control is the low bandwidth of the communication system which, when performing complex tasks, can make the computationally burdening control algorithms impractical in real world scenarios. The other significant limitation is due to the complexity of fully determining the dynamics of the vehicle in water; this makes it hard to perform an accurate parameter identification of the vehicle. In particular, thruster modeling may be problematic due to the non-linearities arising in propeller-vehicle interactions and cross flow-propeller interactions [3].

This work was jointly supported by the EU Commission in the frame of the CFD-OctoProp Project FP7 European Reintegration Grant and the Foundation Grant project PoseiDRONE of the Cassa di Risparmi di Livorno.

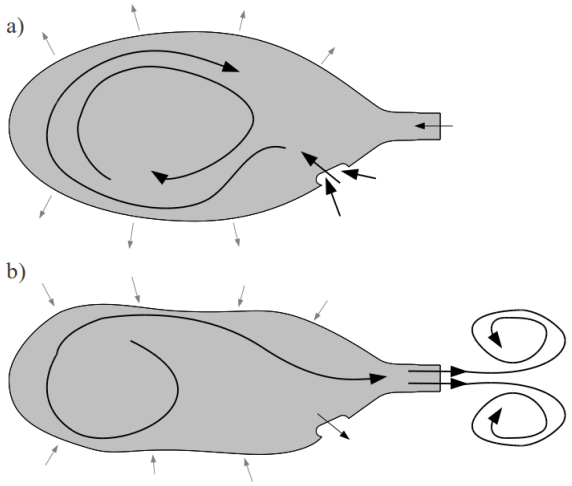

Fig. 1. Lateral view of the working cycle of inflation (a) and collapse (b) and hence, ingestion (a) and expulsion (b) of fluid, for a pulsed-jet propelling organism.

In this paper we present a new kind of underwater vehicle which is composed for 96% of its volume of soft elastomeric materials. By virtue of its highly compliant structure, this Soft Unmanned Underwater Vehicle (SUUV) is capable of undergoing large deformations and remain unaffected by impacts. In addition, the SUUV exploits a thrust production routine which benefits from the highly-deforming morphology and does not suffer from the hindrances occurring with propellers.

II. The Advantages of Soft Unmanned Underwater Vehicles

In the attempt to better address the challenges of complex underwater operations, engineers and scientists have started looking at aquatic animals, [4], as a source of inspiration to design robots with enhanced capabilities compared to standard vehicles. Marine animals sport outstanding manoeuvring skills among which fast-start, [5], and close-radius turning are perfect examples of those features which would be regarded as extremely valuable in underwater robots. In this paper it

978-0-933957-40-4 ©2013 MTS

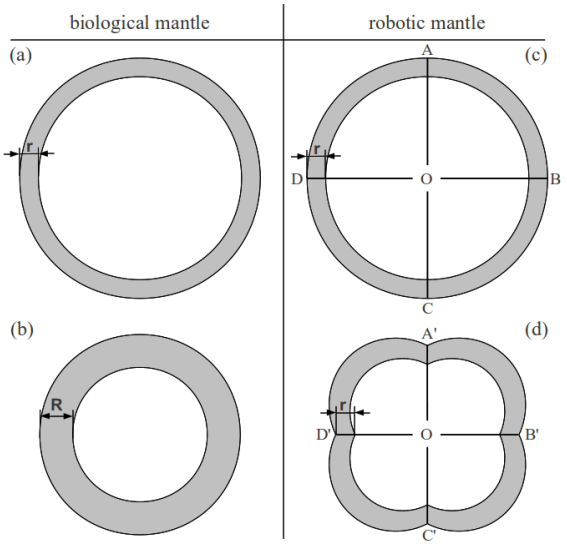

Fig. 2. Cross sectional view of the mantle of a chephalopod during inflation (a) and collpase (b), and the artificial mantle of a SUUV during cable-driven collapse (d) and passive elastic inflation (c).

is argued that an underwater vehicle that exhibits both a high structural compliance and the same degree of manoeuvrability encountered in certain marine animals could virtually constitute the ideal underwater robot to deal with a very broad range of tasks.

In designing a soft-bodied underwater robot, the most obvious source of inspiration lies in cephalopods (*i.e.* squids, octopuses, cuttlefish), [7]. These creatures sport a variety of outstanding swimming capabilities which range from fast-start escape-jetting, to long distance pelagic steadily sustained swimming, to precise manoeuvring for benthonic exploration and hunting. All this is achieved without the support of a proper skeletal structure, of which cephalopods are almost entirely devoid, [6].

Cephalopods rely on pulsed-jet propulsion to thrust themselves through water. This swimming strategy is based on a routine (see Fig. 1) of sequential ingestion and expulsion of finite slugs of water stored in a cavity, the mantle chamber, driven by the contraction of radial (see Fig. 2.b) and circumferential (see Fig. 2.a) muscles of the mantle, [6]. Inflow of ambient water occurs across the ingestion valves (*pallial valves*), while expulsion is driven across a nozzle (*siphon*), Fig. 1.

There are at least two extremely advantageous elements intrinsic to this mode of thrust-producing routine. First, a vast literature has highlighted the association of pulsed-jetting with the formation of circulation-rich, ordered, toroidal, vortical structures, which, in turn, are responsible for an augmented thrust compared to the case of a continuous jet (see [11], [8], [9], [10], [12], [13], [14]). In the second place, recent advancement have proved that isotropic contraction of the mantle volume guarantees further thrust production via the recovery of the kinetic energy associated to the variation of added mass which occurs during this shape change [15]. In addition, it appears that the boundary layer forming over shrinking bodies participates in annihilating part of the effect due to separation otherwise generated, thus contributing to the reduction of the drag acting upon the body, [15].

Given these premises, the authors have developed a working prototype of a soft-bodied underwater vehicle capable of replicating the inflation/deflation routine of cephalopods [16],[17], thus exploiting the series of benefits mentioned above. In this paper the focus is placed in designing a revised version of the existing prototypes of Soft Unmanned Underwater Vehicles. The prototypes presented in [16] and [17] suffered mainly from the limited amount of volume which they were able to expel and from the slow inflation time, which inhibited the process of refill of the mantle cavity, hence depleting the thrust at higher pulsation frequencies. Here we present a new prototype based on the same actuation principle as those already developed, but with a series of improvements which enable the expulsion of the entire volume stored in the mantle cavity and at the same time speed up the refill process. In the reminder of this paper we briefly recall the actuation principle employed in SUUVs and highlight the novelty of the latest prototype presented here. Then a series of tests performed in a controlled environment are described and compared with the performance of the earlier prototypes.

III. Vehicle Design and Actuation

The vehicle travels in water by means of a propulsion strategy resemblant to that of cephalopods. In actual cephalopods, the collapse of the mantle, and hence the pressurization of the internal fluid, occurs by means of the contraction of the circumferential muscles within the mantle thickness. During the shortening of the circumferential muscles, the radial muscles are stretched and the thickness of the mantle wall increases. Then, when the time comes to refill the cavity, the radial muscles contract and in doing so the chamber

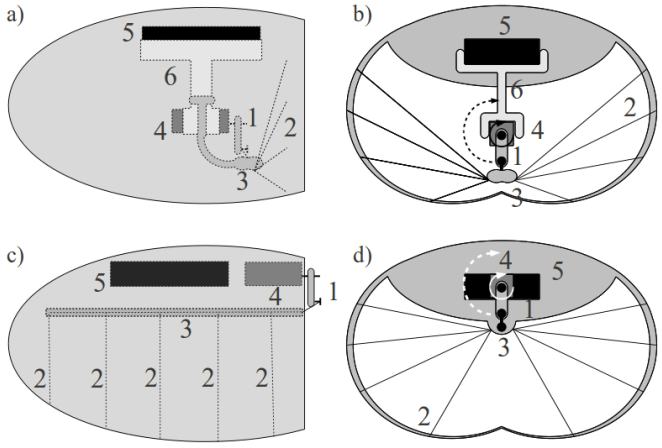

Fig. 3. The difference in the actuator arrangement between the first (a)-(b) and the present (c)-(d) version of the SUUV: (a), (c) lateral and (b), (d) cross sectional view. The numbers in each plot refer to: (1) the crank, (2) the cables, (3) the fairlead, (4) the motor, (5) the batteries, (6) the motor-batteries holding structure.

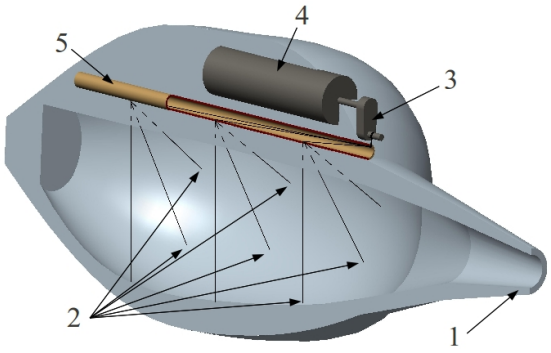

Fig. 4. The Soft Unmanned Underwater Vehicle; numbers refer to: (1) the nozzle, (2) the cable attachment points, (3) the crank, (4) the motor, (5) the axial fairlead.

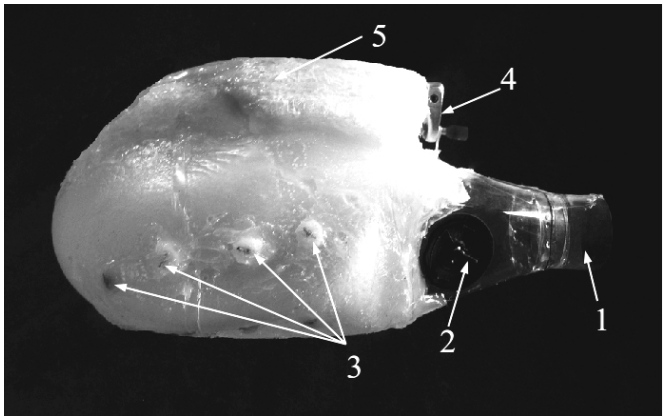

Fig. 5. Lateral view of the Soft Unmanned Underwater Vehicle; numbers refer to: (1) the nozzle, (2) inflow valves, (3) the cable attachment points, (4) the crank, (5) the motor and buoyancy adjustment device housing.

inflates, sucking water inside from the ambient. The actuation principle resembles this working routine by relying on cable transmission driven by a crank mechanism. The compression of the artificial mantle chamber is guided by the shortening of a series of cables fitted, at one end, to the elastic walls of the mantle and, at the other end, to a crank the rotation of which cyclically pulls and releases the cables. In Fig. 2, the difference between the biological working routine and the artificial one are compared. In Fig. 2.c-d it is imagined that four cables with attachment points equispaced one with respect to the other over one cross section are pulled from a spot coinciding with the axis of the cavity. The inward displacement of the attachment points drives the lobe-shaped deformation of the cavity which in turns brings the internal fluid under pressure, accelerating it through the nozzle. The refill phase, on the other hand, occurs passively by exploiting the rigidity of the material which composes the elastic shell. The stresses generated within the elastic walls during the straining by the cables drives the spontaneous inflation of the chamber once the cables are left loose by the crank.

This cable arrangement is regarded favourable compared to a circumferential arrangement within the shell walls. In a circumferentially oriented configuration the tension on the cable during the coiling would be significantly higher than in the case of the radially arranged configuration because the silicone walls would have to be compressed in the direction tangential to the cable. Such arrangement would also affect the capability of the silicone walls to return to the unstrained state due to the friction between the cables and the silicone. The preference for a discrete, radially oriented, cable arrangement is thus motivated by the lower load torque needed for the crank mechanism to execute the collapse of the elastic shell and, at the same time, by the eased passive recovery of the inflated state of the mantle.

In the earlier series of prototypes, the crank mechanism driving the contraction of the cables was located at the centre of the mantle cavity and the cables were gathered through a fairlead in order to equally distribute the contraction among all cables regardless of their point of attachment, see Fig. 3.a-b. For a detailed description of this mechanism, the reader is referred to [16]. This design is improved here by shifting the crank mechanism outside of the hollow cavity and lodging the motor inside the silicone mould. The fairlead is substituted with a tubular structure axially oriented to the body of the vehicle which gathers the cables coming from several cross sections and guiding them across the whole length of the chamber to the crank, see Fig. 3.c-d and Fig. 4. This improved design helps to distribute the action of the crank over as many cross sections as required in order to achieve the maximum pressurization of the chamber.

In its final shape the vehicle, Fig. 5, consists of a hollow elastic shell of Smooth-On EcoFlex® 00-30 silicone the compression of which is driven by four groups of four nylon cables arranged over four cross sections along the shell, as schematically depicted in Fig. 4. The cables, shown in Fig. 6, are attached, at one end, to the shell wall, and, at the other end, gathered through the axially oriented fairlead, see Fig. 4, which guides the cables to a crank fitted onto the shaft of a DC motor

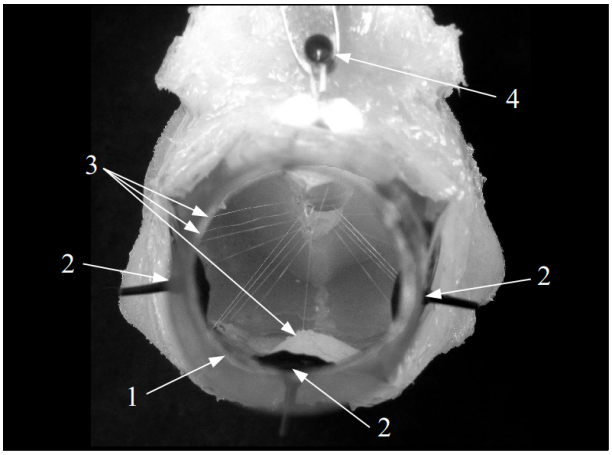

Fig. 6. Front view of the Soft Unmanned Underwater Vehicle across the nozzle; numbers refer to: (1) the nozzle, (2) inflow valves, (3) the cable attachment points, (4) the crank.

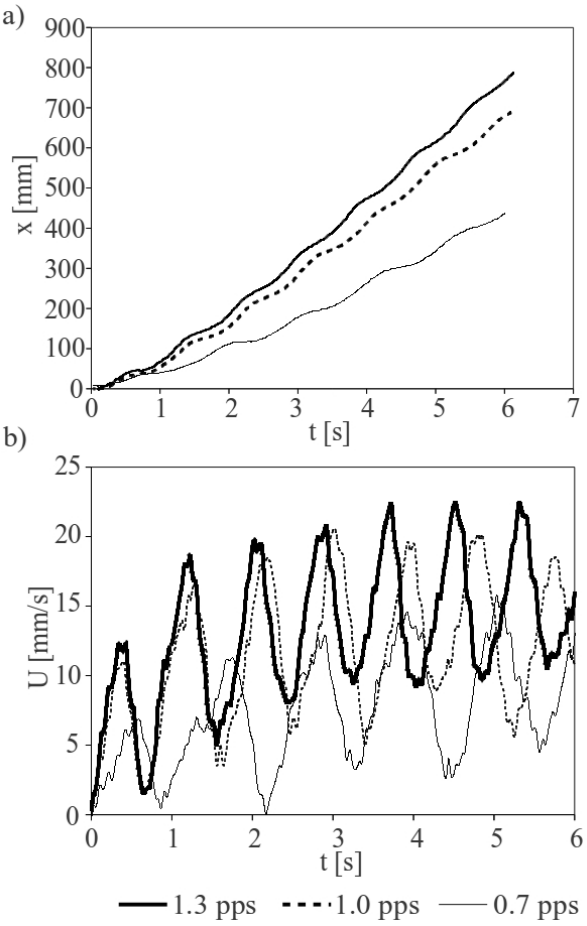

Fig. 7. Temporal profiles of displacement, above, and velocity, below, of the vehicle for tests performed at 0.7, 1.0 and 1.3 pulsation per seconds (pps).

(441435 Maxon Motor), see Fig. 4 and Fig. 6. The nozzle is composed of a cylinder of flexible sheet sealed to the silicone walls and perforated on the side in order to fit three umbrella check valves. These valves are meant to operate in the case when a soft, collapsible nozzle is employed by enabling the inflow of ambient water during the refill phase and preventing the leakage of water during compression of the chamber. In the experiments presented below, however, a rigid nozzle is used therefore the valves are redundant. Finally, in order to speed up the refill process, the shell has been tweaked with a layer of Smooth-On Sil-Poxy silicone adhesive rubber, which drastically contributes to make the walls of the shell more rigid and hence significantly faster at inflating when strained.

IV. Tank Testing

A preliminary set of tests is presented in order to measure the translational speed of the vehicle. The experiments are performed in a 1150 mm long, 590 mm wide and 500 mm deep tank filled with tap water. The vehicle is allowed to travel along a straight line inside the tank by letting the motor revolve at a constant angular velocity. The tests are recorded with a digital camera at 25 fps and subsequently treated with an image tracking software and a Savitzky-Golay low-pass filter to process the displacement and velocity temporal profiles. Results for three pulsation frequencies, namely 0.7, 1.0 and 1.3 pulsations per seconds (pps), are reported in Fig. 7.

The tests bring evidence of the highly non-stationary behaviour of the thrust producing routine which gives rise to a distinct pattern of peaky oscillations in the velocity profile, fig. 7.b. An interesting data emerges by comparing the averaged velocity achieved with this latest prototype and those recorded in the earlier tests with the previous prototypes, see Fig. 8. The most remarkable features highlighted in Fig. 8 are the significant improvement in performances and a trend which is apparently inverted with respect to earlier ones. The first prototypes showed a clear inverse correlation between pulsation frequency and swimming speed. This was in part motivated by the time required for the shell to re-inflate. The tests performed with the latest prototype manifest a reversed trend, showing that performances improved significantly at higher pulsation frequency.

It is reasonable to expect each profile in the averaged velocity versus pulsation frequencies plot to describe a bell-shaped trend, where the optimal performance coincide with the point where the motor rotates at a speed such that it takes half the time of a full rotation to refill the cavity. Below this point, performances increase, and beyond they decrease, because the shell does not have enough time to refill and the motor runs idle for a brief time, during which thrust is not produced. It can be expected that the data from the latest experiments lie in the increasing performance branch of their respective bell, while the earlier tests lie in the decreasing performance side of their own bell. Further testing is required in this respect in order to gain a better insight of the parameters which enable attainment and enhancement of the optimal performance.

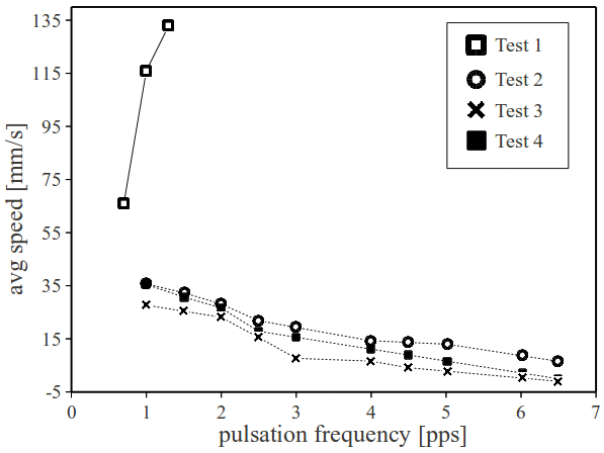

Fig. 8. Profiles of averaged speed of the vehicle [mm/s] versus frequency of pulsation [pps]. All data from the tests performed with the earlier prototype ([16]) lie in the lower part of the plot (decreasing trend), while those tests performed with the new prototype lie in the upper part of the plot (increasing trend). The tests correspond to: Test1, the vehicle presented in this paper, Test2, first prototype with a rigid 30 mm nozzle, Test3, first prototype with a soft 30 mm nozzle, Test4, first prototype with a rigid 14 mm nozzle.

V. Conclusion

A revised design of an earlier prototype of a Soft Unmanned Underwater Vehicle is presented which benefits from a series of significant ameliorations. In particular, a major effort has been devoted to augment the amount of volume expelled in each single pulsation cycle and speed up the refill process. These tweaks enable a remarkable improvement in the performance of the vehicle and offer a clearer perspective of the overall performance of this kind of vehicles as a consequence of design parameters. The comparison between the latest data and earlier records suggest the occurrence of a bell-shaped distribution of the average velocity vs pulsation frequency trend regulated, to a major extent, by the interplay of speed of collapse and speed of refill of the shell. The acknowledgement of this relationship among the design parameters highlights the potential for further optimization of the propulsion dynamics via a refined control of the actuation routine.

References

[1] Luis L. Whitcomb, "Underwater robotics: out of the research laboratory and into the field," Robotics and Automation, 2000. Proceedings. ICRA '00. IEEE International Conference on , vol.1, no., pp.709,716 vol.1, 2000.

[2] Gianluca Antonelli, "Underwater Robots, Motion and Force Control of Vehicle-Manipulator Systems", 2nd Edition, Springer Tracts in Advanced Robotics Volume 2, Bruno Sicilinano, Oussama Khatib, Frans Groen, Springer, 2006.

[3] M. Krieg and K. Mohseni, "Dynamic modeling and control of biologically inspired vortex ring thrusters for underwater robot locomotion", IEEE Transactions on robotics, vol. 26, 542-554, 2010.

[4] P.R. Bandyopadhyay, "Trends in Biorobotic Autonomous Undersea Vehicles", IEEE Journal of Oceanic Engineering, vol. 30, 2005.

[5] J. Conte, Y. Modarres-Sadeghi, M.N. Watts., F.S. Hover and M.S. Triantafyllou, "A Fast-Starting Robotic Fish that Accelerates at 40 ms^{-2}", Journal of Bioinspiration and Biomimetics, vol. 5, 2010.

[6] J. M. Gosline and M. E. DeMont, "Jet-propelled swimming squids", Scientific American, 252, 96-103, 1985.

[7] Sangbae Kim and Cecilia Laschi and Barry Trimmer, "Soft robotics: a bioinspired evolution in robotics", Trend in Biotechnology, vol. 31, pp. 287-294, 2013.

[8] P. S. Krueger and M. Gharib, "The significance of vortex ring formation to the impulse and thrust of starting jet", Physics of Fluid, vol. 15, pp. 12711281, 2003.

[9] P. S. Krueger, "An over-pressure correction to the slug model for vortex ring circulation", Journal of Fluid Mechanics, 545, 427-443, 2005.

[10] P. S. Krueger and M. Gharib, "Thrust augmentation and vortex ring evolution in a fully pulsed jet", AIAA Journal, 43, 792-801, 2005.

[11] M. Krieg and K. Mohseni, "Thrust characterization of a bio-inspired vortex ring generator for locomotion of underwater robots", IEEE Journal of Ocean Engineering, vol. 33, 2008.

[12] J.O. Dabiri, "Optimal vortex formation as a unifying principle in biological propulsion", Annual Review of Fluid Mechanics, 41, 17-33, 2009.

[13] A. A. Moslemi and P. S. Krueger, "Propulsive efficiency of a biomorphic pulsed-jet underwater vehicle", Journal of Bioinspiration and Biomimetics, vol. 5, 1-14, 2010.

[14] L. A. Ruiz and R. W. Whittlesey and J. O. Dabiri, "Vortex-enhanced propulsion", Journal of Fluid Mechanics, vol. 668, 5-32, 2011.

[15] G. D. Weymouth and M. S. Trantafyllou, "Ultra-fast escape of a deformable jet-propelled body", Journal of Fluid Mechanics, vol. 721, pp. 36385, 2013.

[16] F. Giorgio Serchi, A. Arienti and C. Laschi, "Biomimetic Vortex Propulsion: Toward the New Paradigm of Soft Unmanned Underwater Vehicles", IEEE/ASME Transactions on Mechatronics, vol. 18, pp. 484-493, 2013.

[17] F. Giorgio Serchi, A. Arienti, I. Baldoli and C. Laschi, "An elastic pulsed-jet thruster for Soft Unmanned Underwater Vehicles", IEEE International Conference on Robotics and Automation, May 6-10, 2013.